Introduction to the receiver function method

Frederik Tilmann (+ material from Rainer Kind)

4D-MB SPP Short Course, 1 February 2018

Outline

1. Introduction
2. Crustal Vp/Vs ratio and Moho depth from stacking of multiples
3. Common Conversion Point Stacks (CCCP)

paired with lecture on seismic anisotropy (Georg Rümpker)

Outline

Target: Imaging subsurface structure, discontinuities

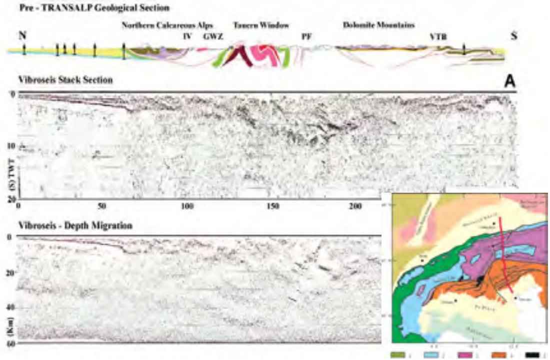

TRANSALP profile Vibroseis+Explosion+passive 1998, 2001 [TRANSALP Working Group, 2002]

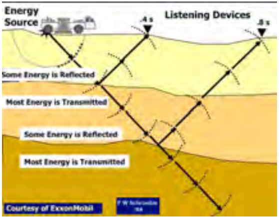

Controlled source reflection seismology:

- Use reflections of P energy
- Method of choice for shallow structure but energy does mostly not penetrate deeply
- No information on S velocity
- Very expensive to carry out

⇒ Use earthquakes as energy source

⇒ The energy is coming from below

⇒ We need to use conversions instead of reflections

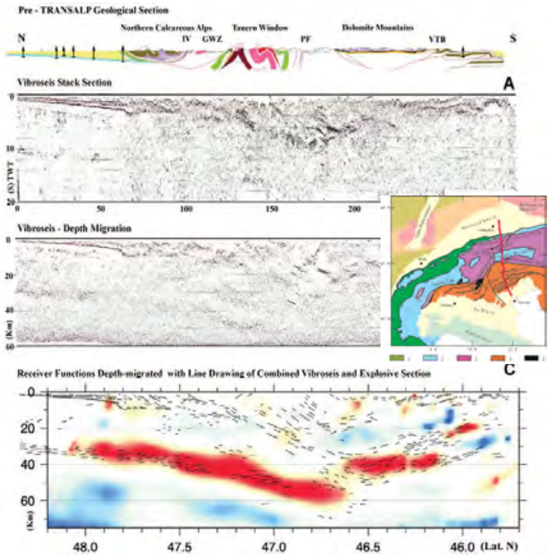

TRANSALP profile Vibroseis+Explosion+passive 1998, 2001 [TRANSALP Working Group, 2002]

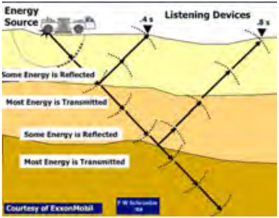

Controlled source reflection seismology:

- Use reflections of P energy
- Method of choice for shallow structure but energy does mostly not penetrate deeply
- No information on S velocity
- Very expensive to carry out

⇒ Use earthquakes as energy source

⇒ The energy is coming from below

⇒ We need to use conversions instead of reflections

Moho depth and Vp/Vs ratios

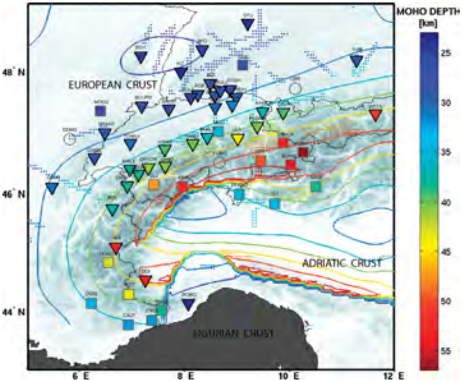

Lombardi et al. [2008]
V_P/V_S varies typically 1.6–2.0, strongly indicative of lithology,
felsic ⇒ mafic implies small ⇒ large V_P/V_S values.

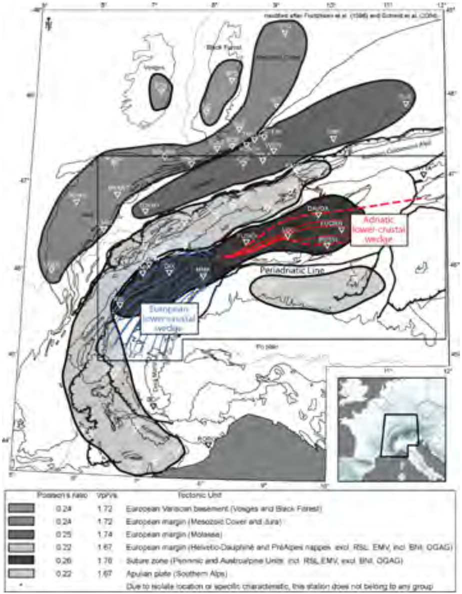

Basics: P and S waves

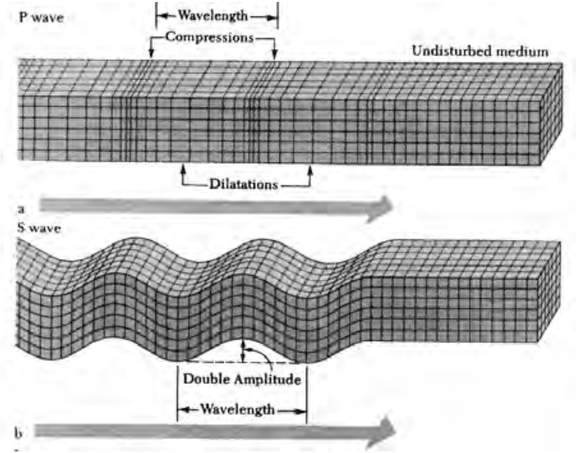

$$V_P = \sqrt{\frac{K + \frac{4}{3}\mu}{\rho}}$$

- K Bulk modulus
- μ Shear modulus
- ρ Density

$$V_S = \sqrt{\frac{\mu}{\rho}}$$

At the same period S wavelength is shorter due to shorter propagation velocity

Basics: P and S waves

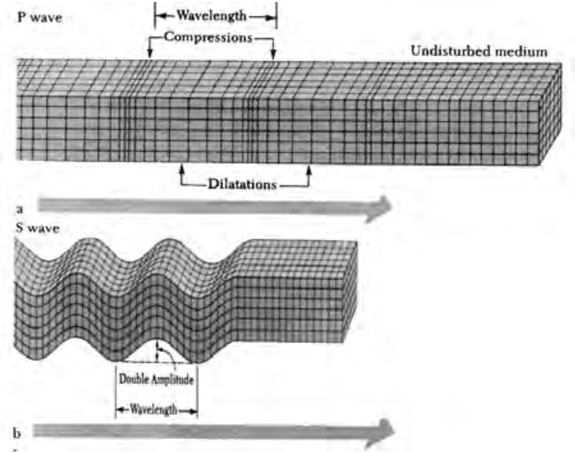

$$V_P = \sqrt{\frac{K + \frac{4}{3}\mu}{\rho}}$$

- K Bulk modulus
- μ Shear modulus
- ρ Density

$$V_S = \sqrt{\frac{\mu}{\rho}}$$

At the same period S wavelength is shorter due to shorter propagation velocity

P and S wave: interaction with interface

- Incident P ⇒ converted SV wave (except when exactly vertically incident)
- No SH wave (T component) converted by flat interface
- Also works the other way round: incident SV ⇒ converted P

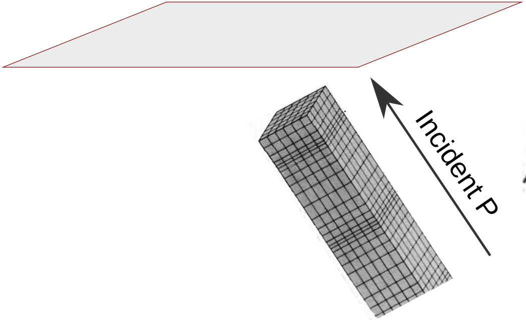

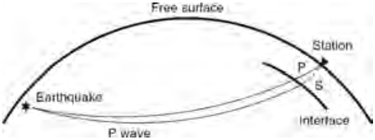

Note that in reality the different types of motion overlap and affect the same volume.

P and S wave: interaction with interface

- Incident P ⇒ converted SV wave (except when exactly vertically incident)
- No SH wave (T component) converted by flat interface
- Also works the other way round: incident SV ⇒ converted P

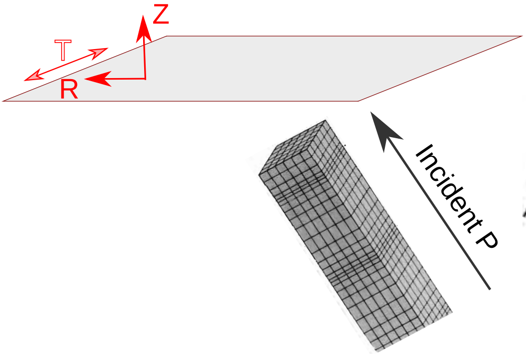

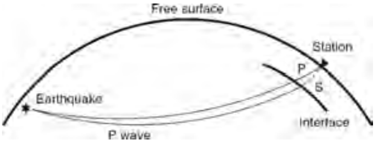

Note that in reality the different types of motion overlap and affect the same volume.

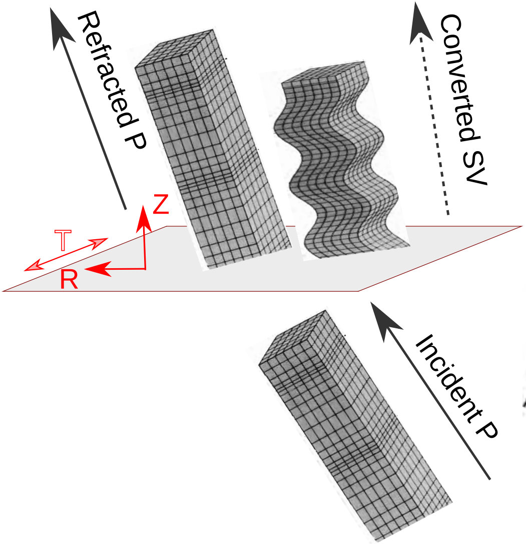

- Incident P ⇒ converted SV wave (except when exactly vertically incident)
- No SH wave (T component) converted by flat interface
- Also works the other way round: incident SV ⇒ converted P

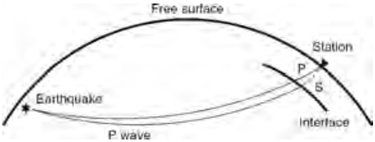

Note that in reality the different types of motion overlap and affect the same volume.

P and S wave: interaction with interface

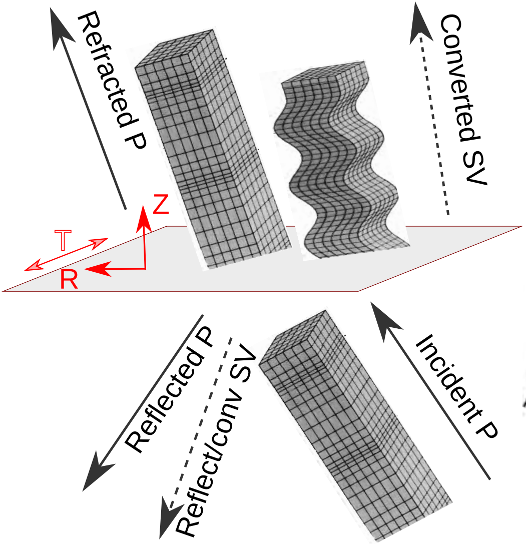

- Incident P ⇒ converted SV wave (except when exactly vertically incident)
- No SH wave (T component) converted by flat interface
- Also works the other way round: incident SV ⇒ converted P

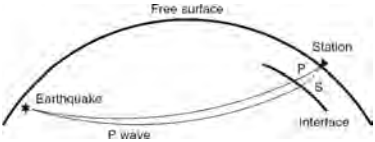

Note that in reality the different types of motion overlap and affect the same volume.

P and S wave: interaction with interface

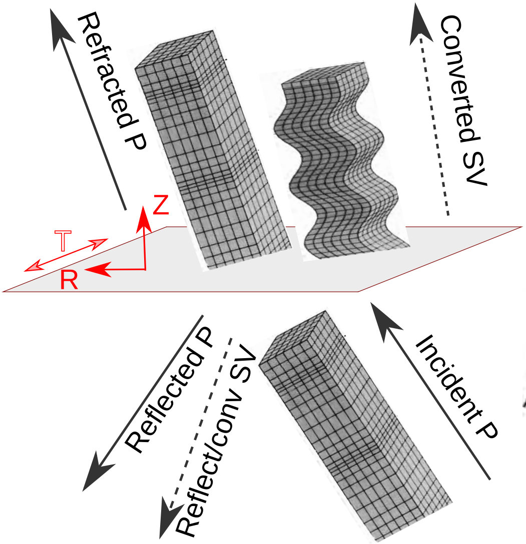

- Incident P ⇒ converted SV wave (except when exactly vertically incident)
- No SH wave (T component) converted by flat interface
- Also works the other way round: incident SV ⇒ converted P

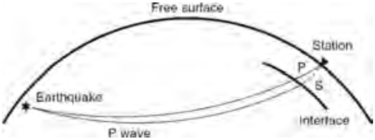

Note that in reality the different types of motion overlap and affect the same volume.

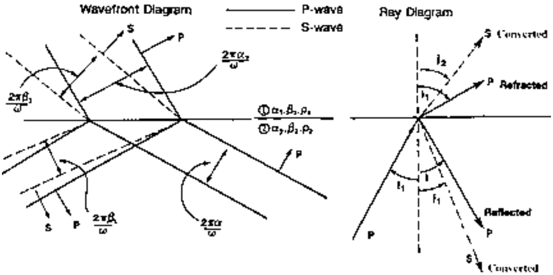

Wavefronts along interface need to stay in phase: ⇒ Snell's law: $\frac{\sin \iota_{1P}}{V_P} = \frac{\sin \iota_{2S}}{V_S}$
⇒ Converted S waves propagate more steeply than their originating P waves

Using RF for imaging discontinuity depths

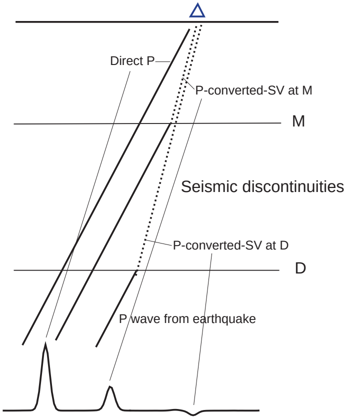

Use time-separation of waves converted from P-to-S at discontinuities underneath the receiver.

Take home

Interface with velocity increase with depth shows up as positive wiggle, velocity decrease as negative wiggle.

Fast-to-slow (e.g. Moho)

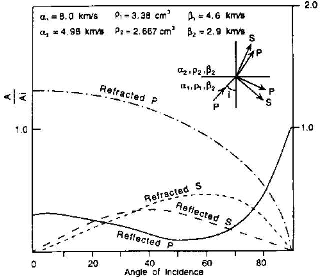

Slow-to-fast (e.g. magma chamber, LAB)

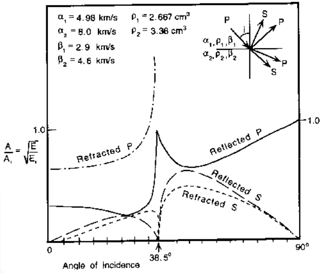

Using RF for imaging discontinuity depths

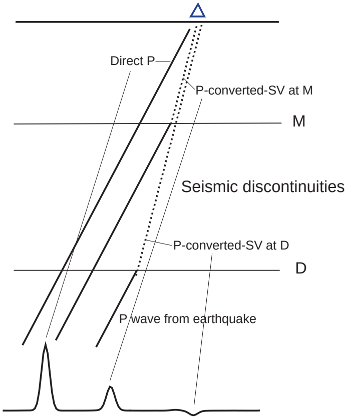

Fast-to-slow (e.g. Moho)

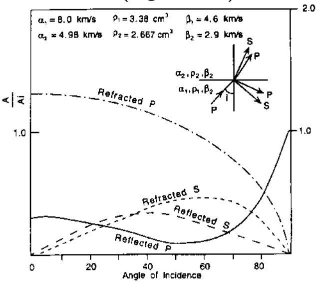

Slow-to-fast (e.g. magma chamber, LAB)

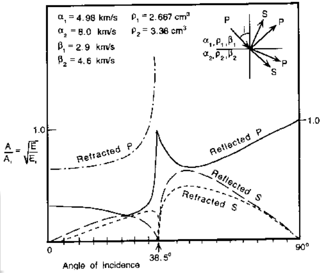

Use time-separation of waves converted from P-to-S at discontinuities underneath the receiver.

Take home

Interface with velocity increase with depth shows up as positive wiggle, velocity decrease as negative wiggle.

Diffractions

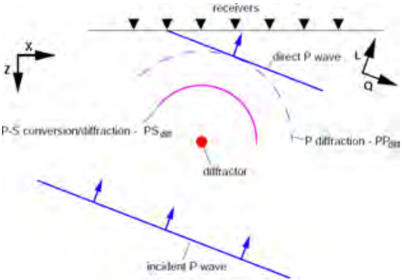

Ryberg&Weber (2000)

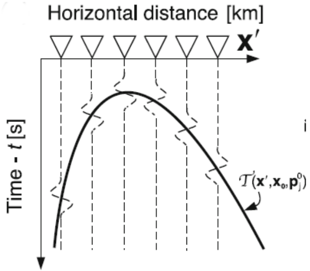

Rondenay [2009]

Anything that is not a smooth horizontal interface will give rise to diffractions, in particular also topography of any interface.

Incident P wave in a simple crust

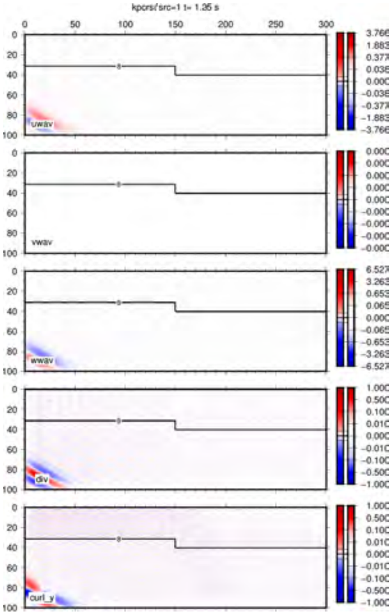

R component (SV+P)

T component (SH)

Z component (P+SV)

P (norm.)

SV (norm.)

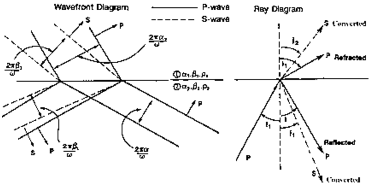

Incident P wave in a simple crust

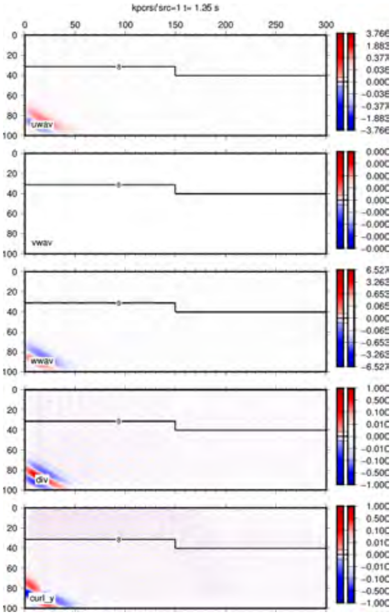

R component (SV+P)

T component (SH)

Z component (P+SV)

P (norm.)

SV (norm.)

What are multiples?

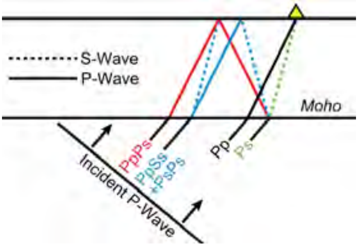

Fig: A. Frassetto

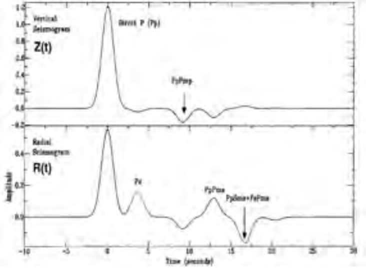

NB: such a clean signal is rarely achieved

P- and S-receiver functions

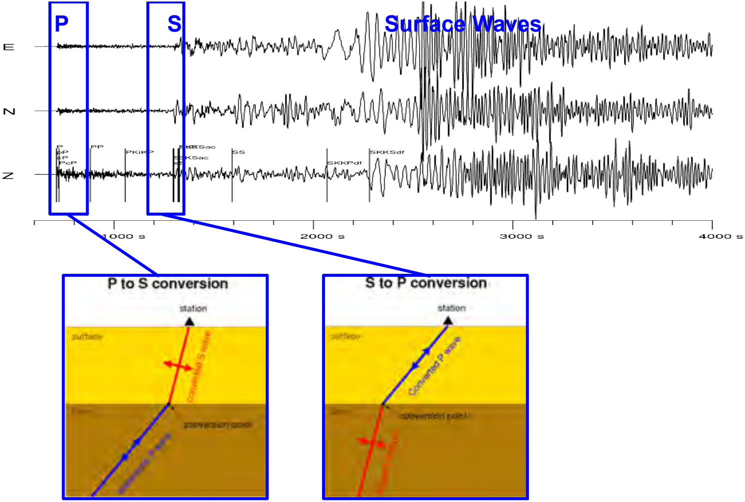

The making of a *receiver function*

Multiple effects build the seismograms

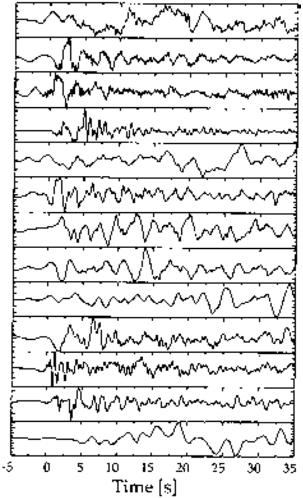

R component traces at station in Australia

[Kennett, 2002]

<u>But:</u> the conversions are hard to see in raw data because in addition to the sequence of interfaces, the seismograms are influenced by

- Instrument response
- Source complexity
- Near-source structure (e.g. surface reflections)

Each effect is combined with the others by a process called convolution.
Here, We are interested in <u>receiver</u> structure
⇒ we do not need to know these effects in detail.

Refresher: convolution and deconvolution

Noise-free synthetic data ($T_0 = 10$s)

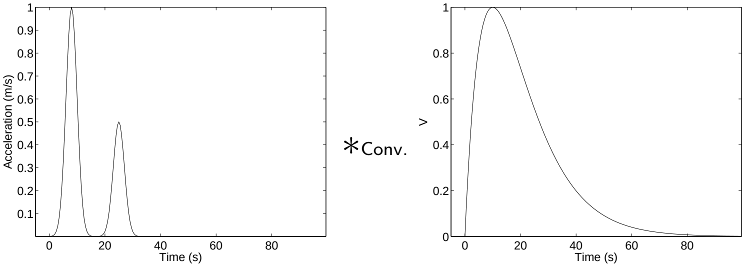

NB Deconvolution is inherently unstable and needs to be regularised (different methods available)!

Aster et al. [2005]

Refresher: convolution and deconvolution

Noise-free synthetic data ($T_0 = 10$s)

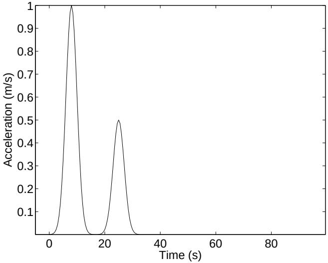

$*$Conv.

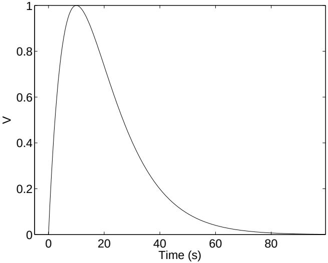

$\Rightarrow$

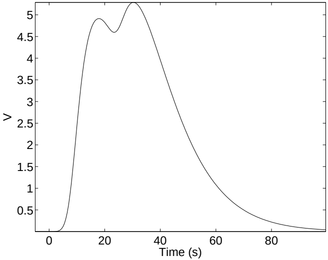

$\overrightarrow{\text{Decon}}$

NB Deconvolution is inherently unstable and needs to be regularised (different methods available)!

Aster et al. [2005]

Refresher: convolution and deconvolution

Noise-free synthetic data ($T_0 = 10$s)

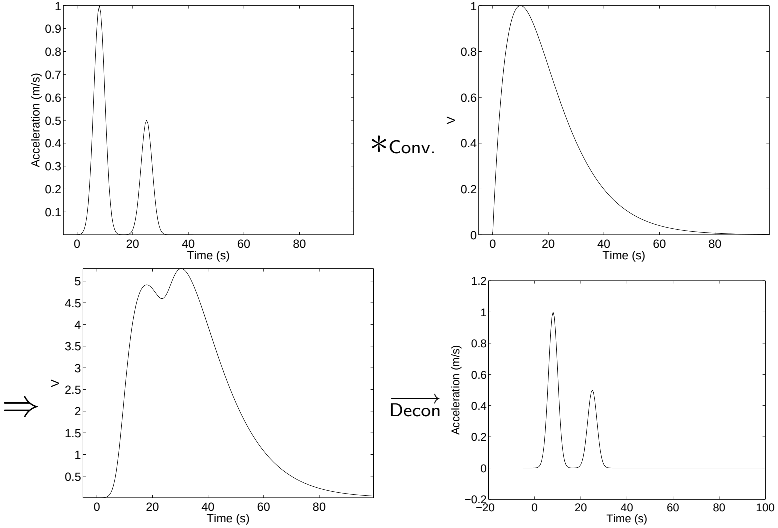

NB Deconvolution is inherently unstable and needs to be regularised (different methods available)!

Aster et al. [2005]

Refresher: convolution and deconvolution

Noisy synthetic data ($T_0 = 10$s)

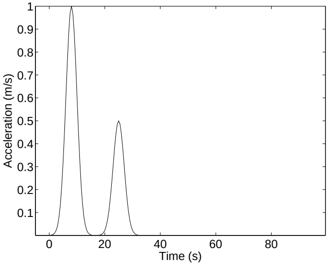

$*$Conv.

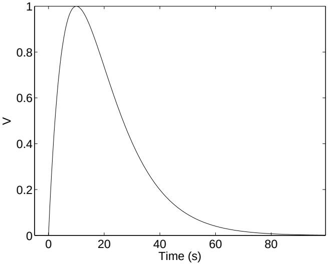

$\Rightarrow$

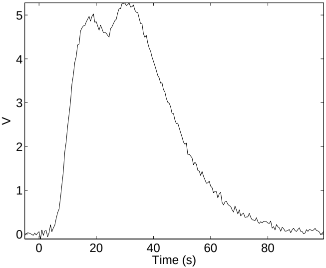

$\xrightarrow{\text{Decon}}$

NB Deconvolution is inherently unstable and needs to be regularised (different methods available)!

Aster et al. [2005]

Refresher: convolution and deconvolution

Noisy synthetic data ($T_0 = 10$s)

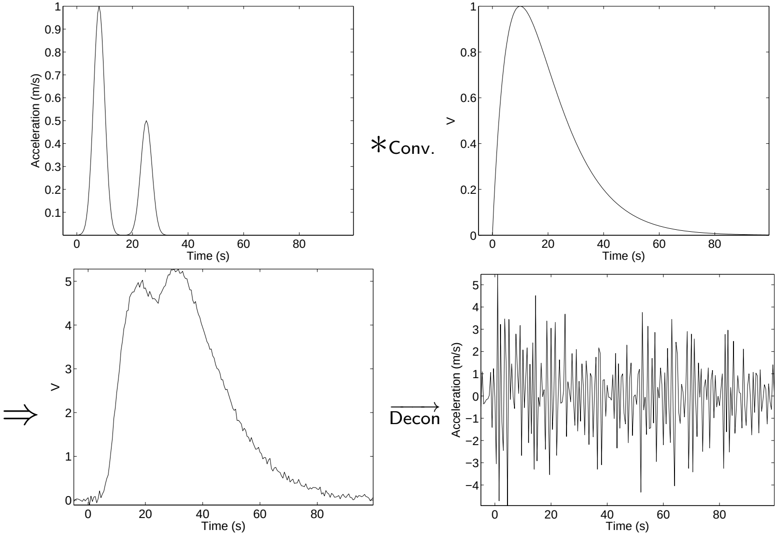

NB Deconvolution is inherently unstable and needs to be regularised (different methods available)!

Aster et al. [2005]

Refresher: convolution and deconvolution

Noisy synthetic data ($T_0 = 10$s)

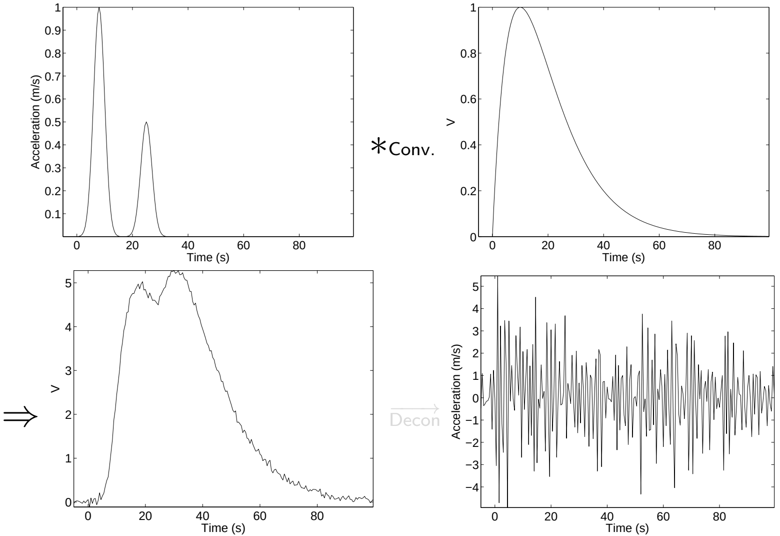

NB Deconvolution is inherently unstable and needs to be regularised (different methods available)!

Aster et al. [2005]

The making of a *receiver function*

Isolating the receiver effect by deconvolution

The ‘receiver function’ idea: Use the P wave as proxy for the incident wave signature (source$*$ near source$*$mantle propagation$*$instrument) [Vinnik, 1977, Langston, 1979].

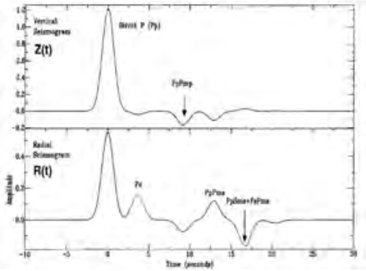

Deconvolve vertical component from radial component to obtain RF

The making of a *receiver function*

Isolating the receiver effect by deconvolution

The ‘receiver function’ idea: Use the P wave as proxy for the incident wave signature (source$*$ near source$*$mantle propagation$*$instrument) [Vinnik, 1977, Langston, 1979].

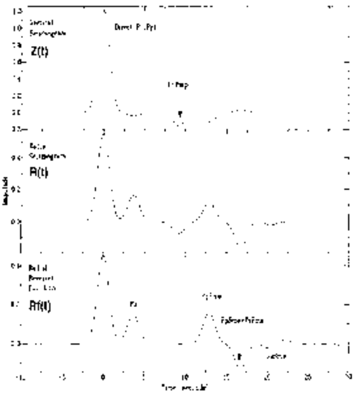

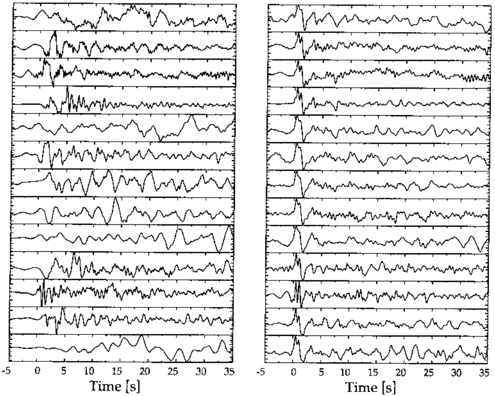

Deconvolve vertical component from radial component to obtain RF

The making of a *receiver function*

Isolating the receiver effect by deconvolution

The 'receiver function' idea: Use the P wave as proxy for the incident wave signature (source$*$ near source$*$mantle propagation$*$instrument) [Vinnik, 1977, Langston, 1979].

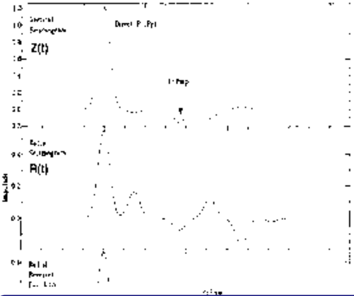

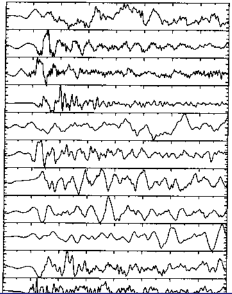

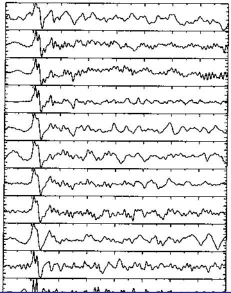

Deconvolution

Deconvolution - division in freq domain (fourier transformed time series)

$$Rf(\omega) = c(\omega)\frac{R(\omega)}{Z(\omega)}$$

The deconvolution removes source and instrument effects (cancel in division)
$\Rightarrow$ RF is only dependent on the structure below receiver and incidence angle

The making of a *receiver function*

Variants: component decomposition

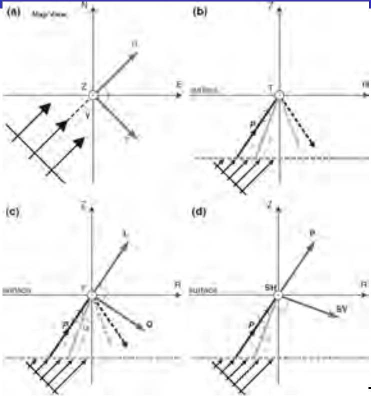

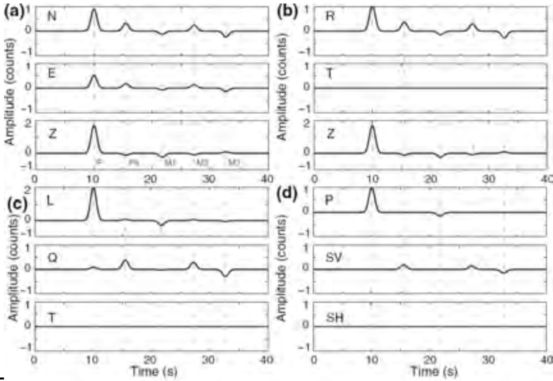

[Rondenay, 2009]

Deconvolve Z from R, or L from Q.

The making of a *receiver function*

Variants: component decomposition

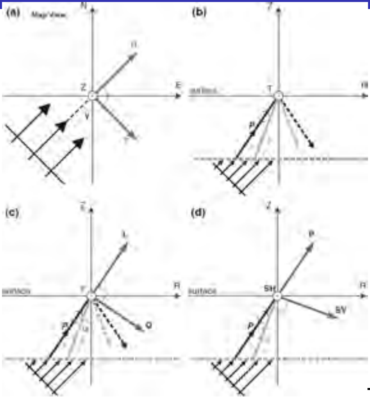

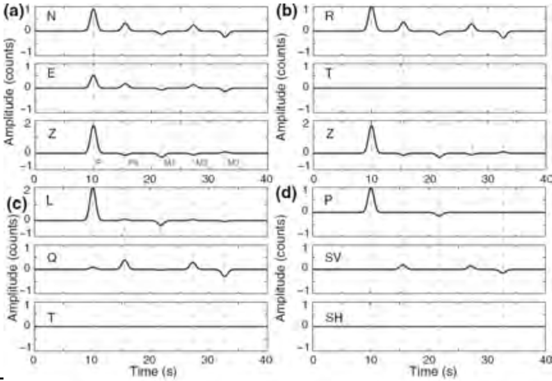

Take-home

ZRT RF will have large peak at 0 s/0 km. Sedimentary basins can lead to a slight shift of

LQT RF will have nearly zero amplitude at 0 s/0 km. In presence of thick sediments, strong amplitudes near 0 km / 0 s.

For deeper structures no strong difference between both methods.

P- and S receiver functions

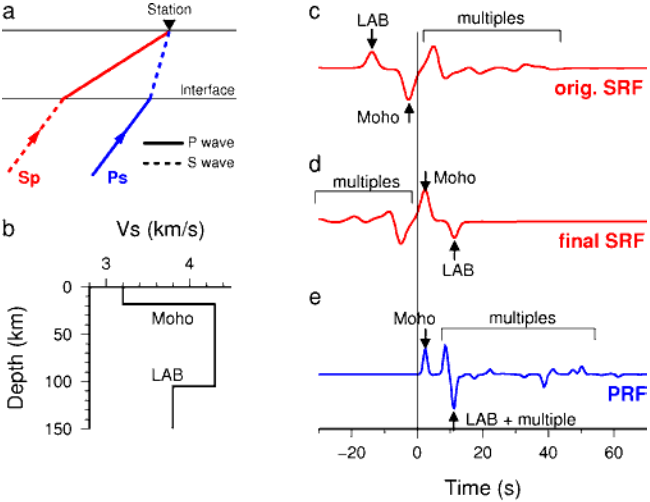

- Crustal multiples in P-RF obscure mantle discontinuities
- As conversion appear before main phase, this does not affect S-RF (but higher noise level, lower frequency, potential contamination by other phases)

Outline

Moveout of direct phases and multiples

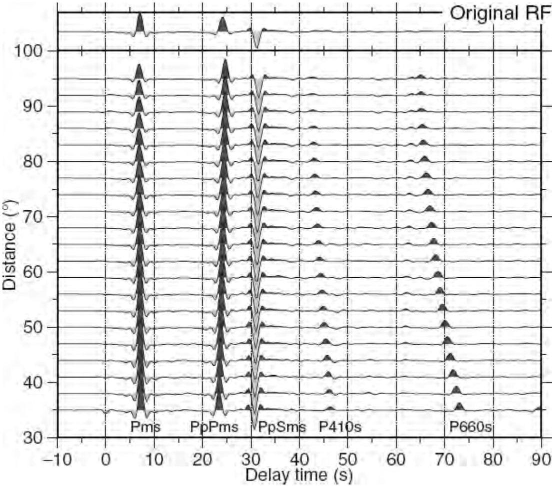

[Kind and Yuan, 2011]

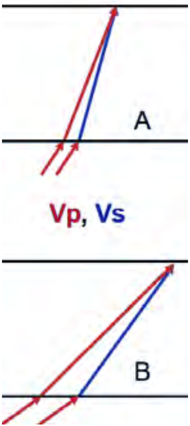

Fig: A. Frassetto

$H - \kappa$ stacking method

Introduced by Zhu [2000] – $\kappa = V_P/V_S$

Observables:

$$
\begin{aligned}
\Delta t_{Ps} &= H(\eta_S - \eta_P) && (1)\\
\Delta t_{PpPms} &= h(\eta_S + \eta_P) && (2)\\
\Delta t_{PsPms} &= 2h\eta_S && (3)
\end{aligned}
$$

(Definitions:

$\eta_P = \sqrt{V_P^{-2} - p^2}, \quad \eta_S = \sqrt{V_S^{-2} - p^2}$)

p is given by distance of earthquake

Unknowns:

- H Depth to Moho
- V_P Average P velocity crust
- V_S Average S velocity crust

Redundant equations $\Rightarrow$ only 2 param.can be determined independently.
Usually one fixes V_P and searches for combinations of H and $\kappa = V_P/V_S$ that fit the observed RFs.
Based on trial values, calculate $\Delta t_{PS,PpmS,PsPms}$ and calculate

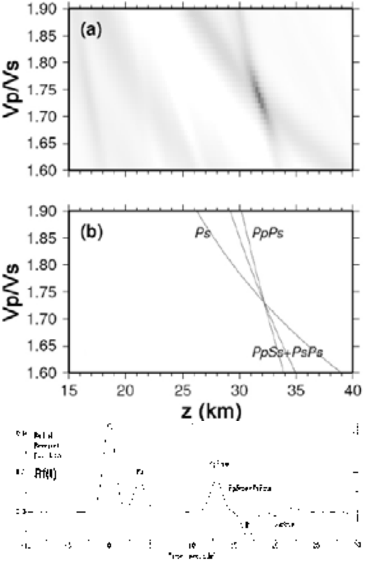

$$A(H,\kappa) = 0.7Rf(\Delta t_{Ps}) + 0.2Rf(\Delta t_{PpPs}) - 0.1Rf(\Delta t_{PpSs})$$

Good data: permanent stations in California

Zhu and Kanamori [2000]

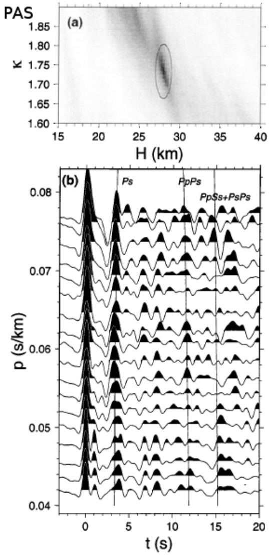

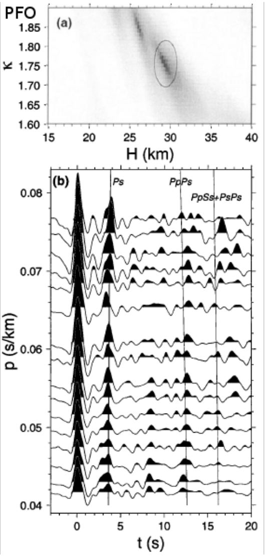

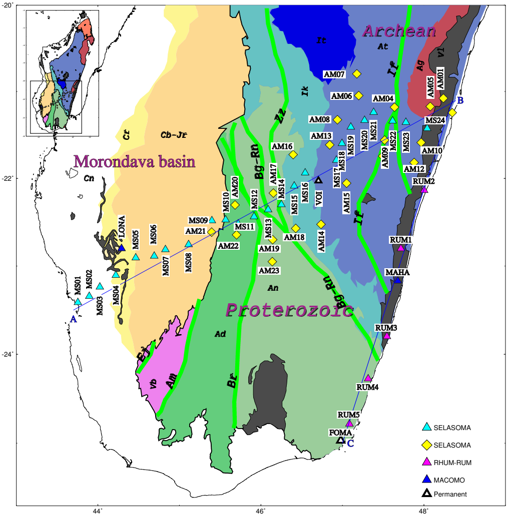

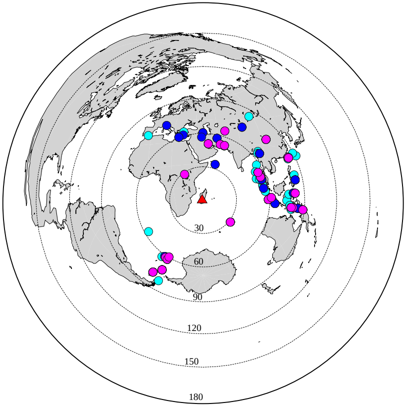

Typical temporary array data (1-2 years deployment)

Case study: SELASOMA profile (Southern Madagascar)

ZR Receiver function stacks

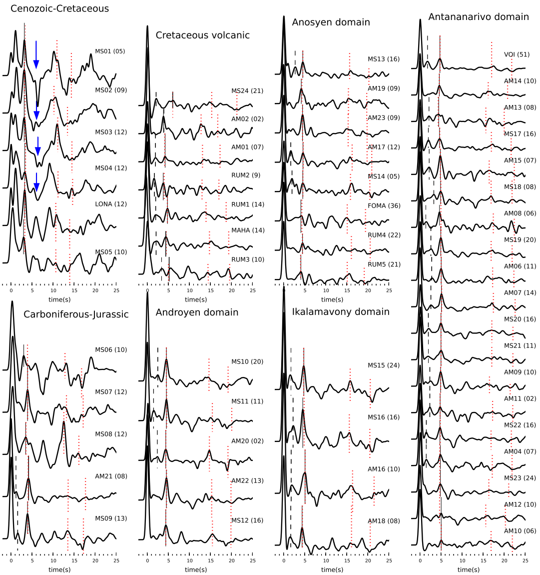

Case study: SELASOMA profile (Southern Madagascar)

ZR Receiver function stacks

Archaean:

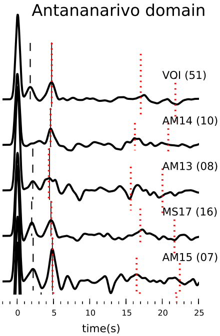

- Direct wave at 0 s
- Clear mid-crustal discontinuity (upper crust/lower crust)
- Clear but relatively weak Moho conversion and multiples

Proterozoic:

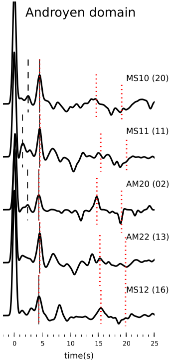

- Direct wave at 0 s
- Only weak conversion from within the crust
- Distinct Moho conversion and (at some stations) multiples

Sedimentary basin:

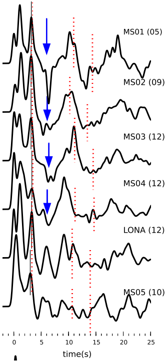

- Strongest peak from sediment basement conversion, not direct wave (at most stations)
- ‘Messier’ RF
- Moho difficult to separate from sediment multiples

Working with less-than-perfect data

What can go wrong?

- Multiples too weak, or scattered in time

  Cause Lateral heterogeneity (dipping boundary, small-scale heterogeneity), gradual transition

  Consequence Result is controlled solely by *Ps* conversion, perfect trade-off, need to assume V_P/V_S ratio to get H or vice versa.

- Ambiguous phase identification

  Cause Most prominent discontinuity might not be the target one (e.g. Moho);

  Consequence Misinterpretation. Completely wrong measurements not representative of either discontinuity can result from interference of multiples.

Precambrian crust - Madagascar [Rindraharisaona et al., 2017]

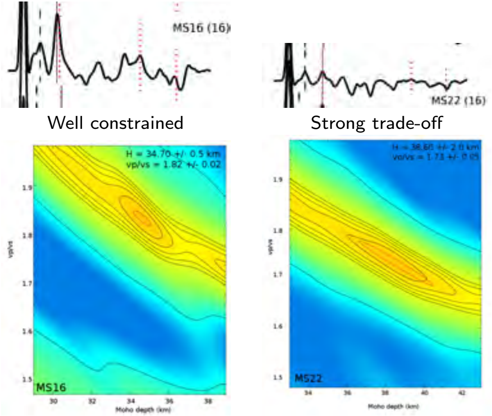

Working with less-than-perfect data

What can go wrong?

- Multiples too weak, or scattered in time

  Cause
  : Lateral heterogeneity (dipping boundary, small-scale heterogeneity), gradual transition

  Consequence
  : Result is controlled solely by *Ps* conversion, perfect trade-off, need to assume V_P/V_S ratio to get H or vice versa.

- Ambiguous phase identification

  Cause
  : Most prominent discontinuity might not be the target one (e.g. Moho);

  Consequence
  : Misinterpretation. Completely wrong measurements not representative of either discontinuity can result from interference of multiples.

Synthetic example [Wölbern and Rümpker, 2017]

Sharp Moho | Transitional Moho

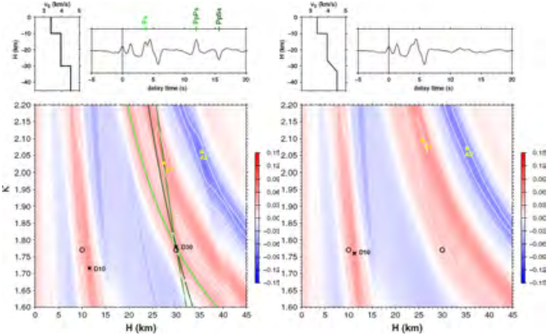

Working with less-than-perfect data

What can go wrong?

- Multiples too weak, or scattered in time

  Cause Lateral heterogeneity (dipping boundary, small-scale heterogeneity), gradual transition

  Consequence Result is controlled solely by *Ps* conversion, perfect trade-off, need to assume V_P/V_S ratio to get H or vice versa.

- Ambiguous phase identification

  Cause Most prominent discontinuity might not be the target one (e.g. Moho);

  Consequence Misinterpretation. Completely wrong measurements not representative of either discontinuity can result from interference of multiples.

Cretaceous volcanics - Madagascar [Rindraharisaona et al., 2017]

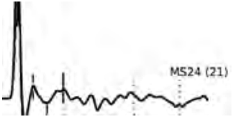

- Multiples too weak, or scattered in time

  Cause Lateral heterogeneity (dipping boundary, small-scale heterogeneity), gradual transition

  Consequence Result is controlled solely by *Ps* conversion, perfect trade-off, need to assume V_P/V_S ratio to get H or vice versa.

- Ambiguous phase identification

  Cause Most prominent discontinuity might not be the target one (e.g. Moho);

  Consequence Misinterpretation. Completely wrong measurements not representative of either discontinuity can result from interference of multiples.

Cretaceous volcanics - Madagascar [Rindraharisaona et al., 2017]

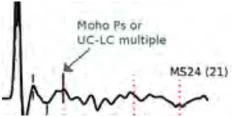

Working with less-than-perfect data

What can go wrong?

- Multiples too weak, or scattered in time

  Cause Lateral heterogeneity (dipping boundary, small-scale heterogeneity), gradual transition

  Consequence Result is controlled solely by *Ps* conversion, perfect trade-off, need to assume V_P/V_S ratio to get H or vice versa.

- Ambiguous phase identification

  Cause Most prominent discontinuity might not be the target one (e.g. Moho);

  Consequence Misinterpretation. Completely wrong measurements not representative of either discontinuity can result from interference of multiples.

Cretaceous volcanics - Madagascar [Rindraharisaona et al., 2017]

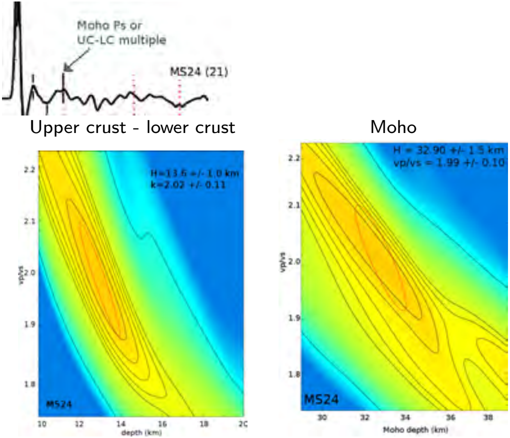

Case study: SELASOMA profile (Southern Madagascar)

Moho depth

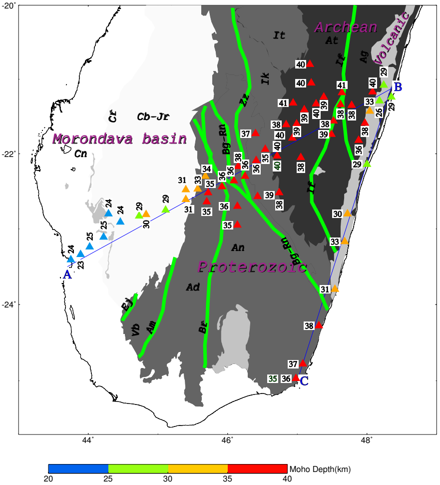

V_P/V_S ratio

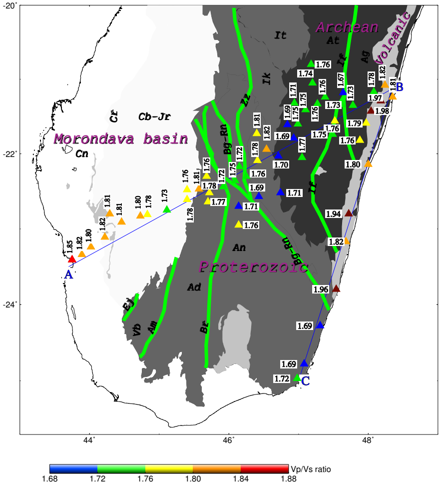

Case study: SELASOMA profile (Southern Madagascar)

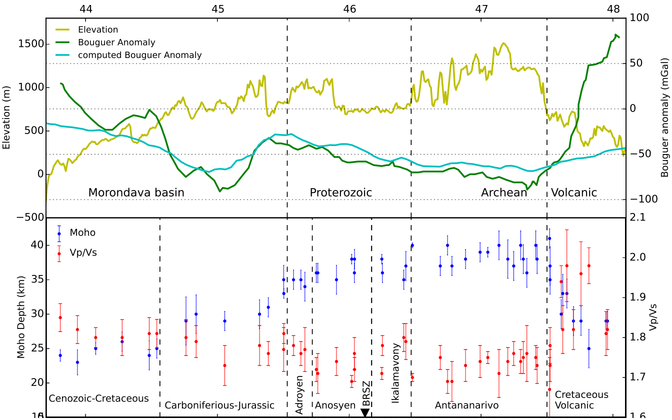

Interpretation

The recovered V_P/V_S represents an whole-crust average - it generally cannot be used to directly identify lithologies but needs to take into account the varying crustal layers but can inform on the dominant bulk composition

NB The V_P/V_S ratio measurement is generally less reliable than Moho depth measurement

Case study: SELASOMA profile (Southern Madagascar)

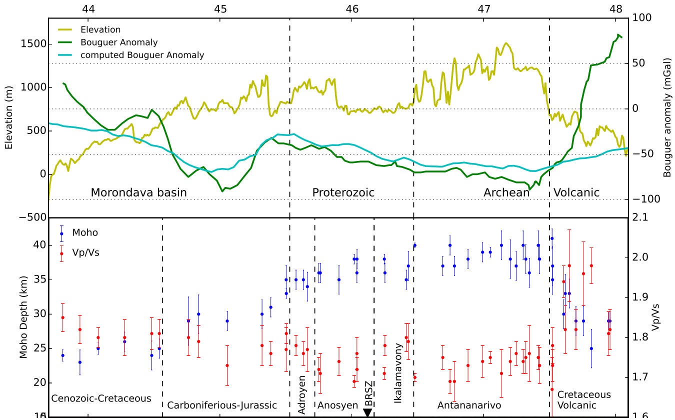

Interpretation

The recovered V_P/V_S represents an whole-crust average - it generally cannot be used to directly identify lithologies but needs to take into account the varying crustal layers but can inform on the dominant bulk composition

NB The V_P/V_S ratio measurement is generally less reliable than Moho depth measurement

Case study: SELASOMA profile (Southern Madagascar)

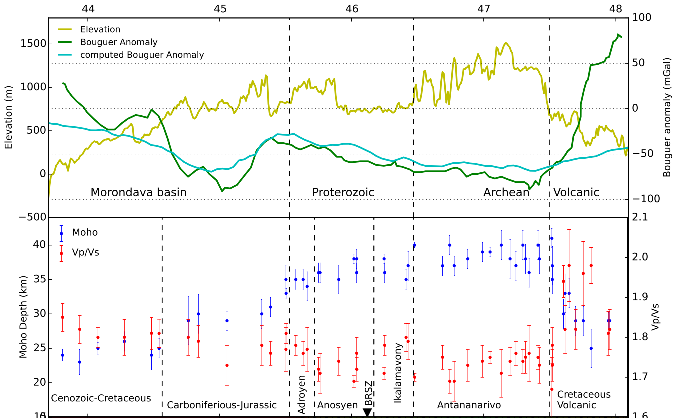

Contributions of crustal layers to bulk V_P/V_S

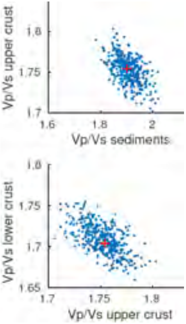

Interpretation

The recovered V_P/V_S represents an whole-crust average - it generally cannot be used to directly identify lithologies but needs to take into account the varying crustal layers but can inform on the dominant bulk composition

NB The V_P/V_S ratio measurement is generally less reliable than Moho depth measurement

Outline

CCCP - Basic principle

Geometry for P-RF

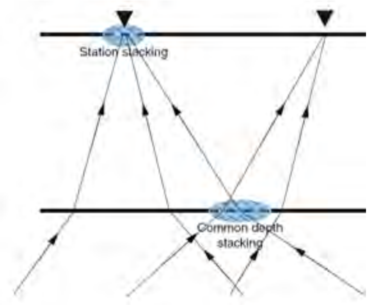

S-RF

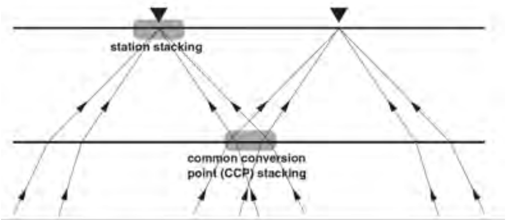

- Assume conversions occur at subhorizontal interfaces
- Write seismogram amplitudes into bins along expected ray path of converted phase

⇒ Ignores diffraction (equiv. to assuming specular reflection in reflection problems)

Synthetic example – One-layer crust (Movie)

Single earthquake

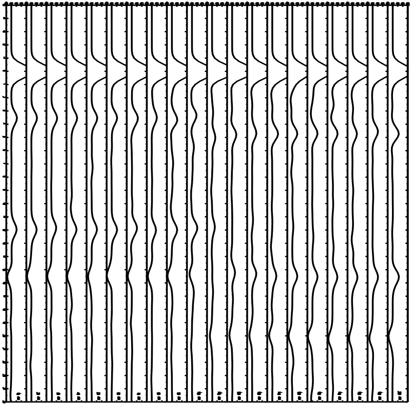

⇒

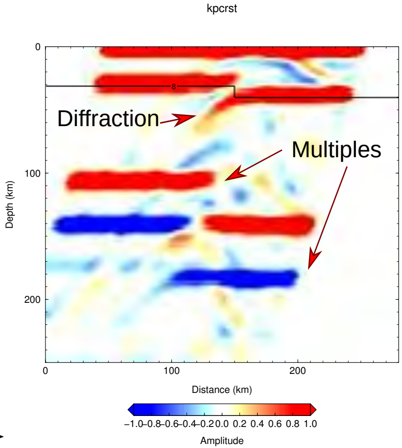

Case study: SELASOMA profile Southern Madagascar

P-RF - Rindraharisaona et al. [2017]

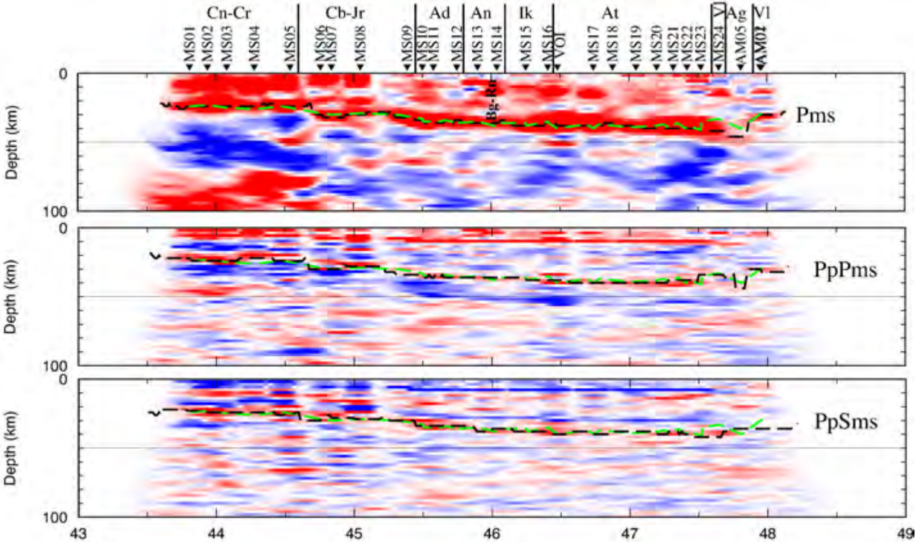

P-RF vs S-RF

Example: Himalaya-Tibet continental collision

P-RF (high frequency):

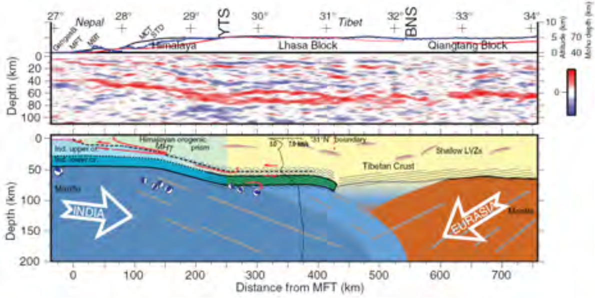

Nábělek et al. [2009]

Detailed images of the crustal interfaces and Moho. Deeper structure obscured by multiples and not shown.

S-RF (low-frequency):

Note that the cross-sections are not exactly from the same profile.

P-RF vs S-RF

Example: Himalaya-Tibet continental collision

P-RF (high frequency):

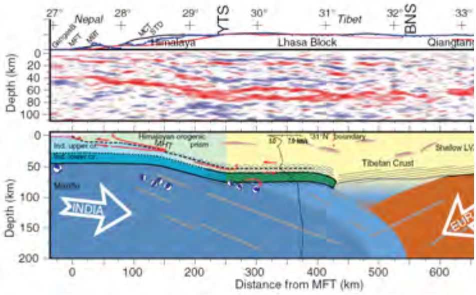

Náběleк et al. [2009]

Detailed images of the crustal interfaces and Moho. Deeper structure obscured by multiples and not shown.

S-RF (low-frequency):

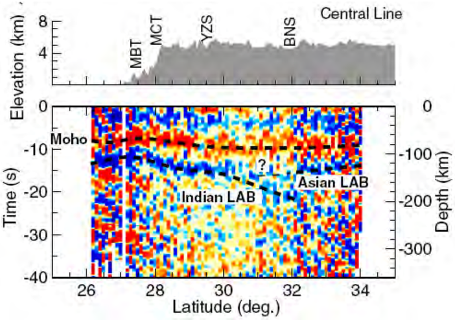

Zhao et al. [2010]

Only low-resolution Moho, no internal crustal structure. Images mantle discontinuties, e.g. LAB (lithosphere-asthenosphere boundary)

Note that the cross-sections are not exactly from the same profile.

P-RF vs S-RF direct comparison

Example: North Chile subduction zone

Time section P-RF vs S-RF

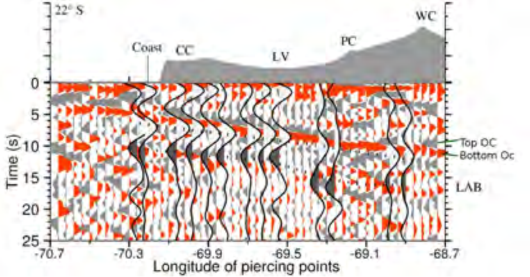

Sodoudi et al. [2011]

For reference: P-RF CCCP

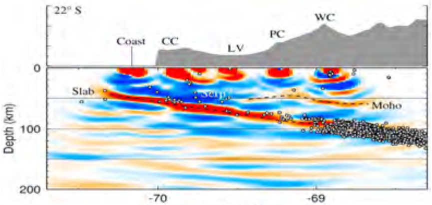

What can go wrong?

Dipping interfaces [Schneider et al., 2013]

PRF - Pamir continental subduction

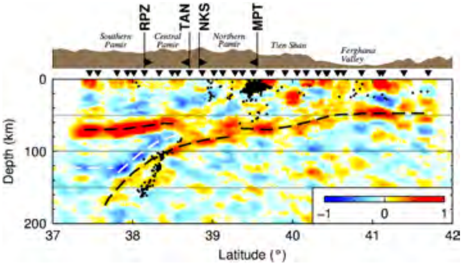

Because the assumption of conversion at horizontal interfaces, dipping structure are shown at too shallow dip (significant effect for dips$>\sim 30^{\circ}$)

Dipping interfaces

Synthetic tests [Schneider et al., 2013]

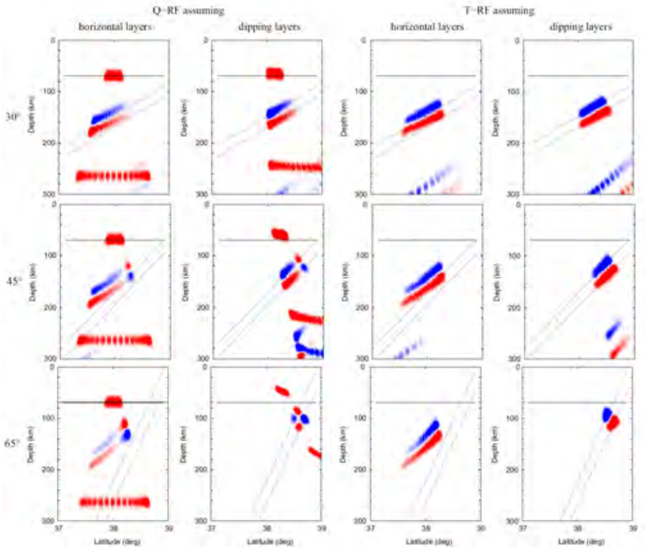

What can go wrong?

Dipping interfaces [Schneider et al., 2013]

PRF - Pamir continental subduction

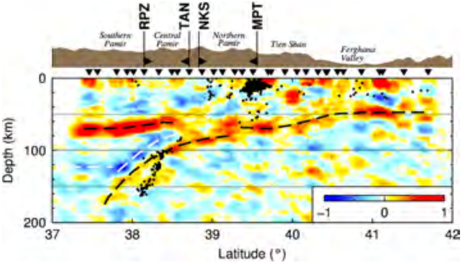

Because the assumption of conversion at horizontal interfaces, dipping structure are shown at too shallow dip (significant effect for dips$>\sim 30^\circ$)

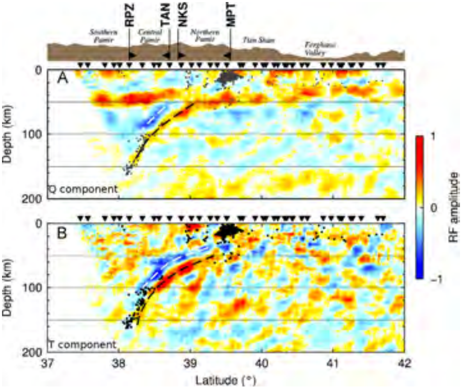

CCCP stacking under assumption of dipping interface images the steeply dipping structure correctly but will show horizontal interfaces (here the flat Moho) more shallow than in reality.

A more general approach: migration

Make no assumptions on smoothness or geometry of discontinuites/anomalies. Trace seismic energy to all possible locations where conversion might have happened. $\Rightarrow$ Constructive interference at real conversion points, destructive interference at all others.

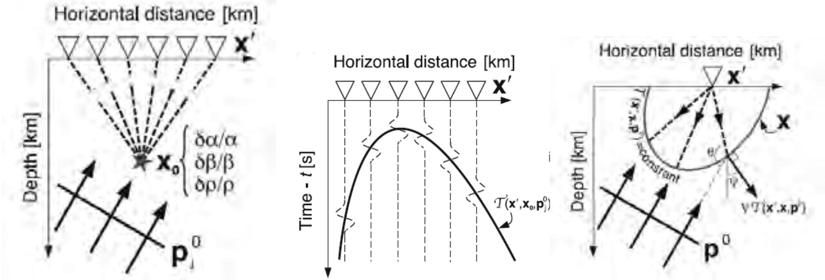

[Rondenay, 2009]

A more general approach: migration
Comparing (horizontal) CCCP to migration

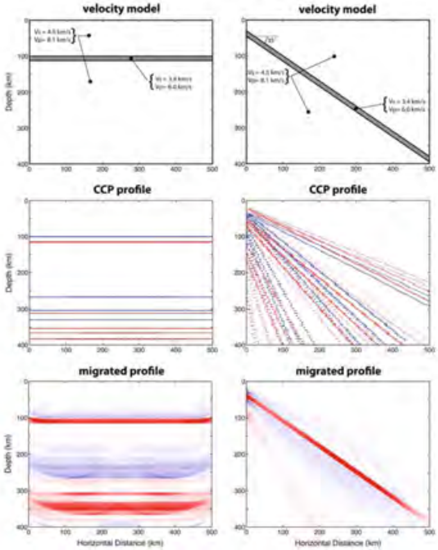

6 in-plane incident waves at different slownesses[Rondenay, 2009]

A more general approach: migration

However:

Requires very good information on velocity model:

Correct velocity

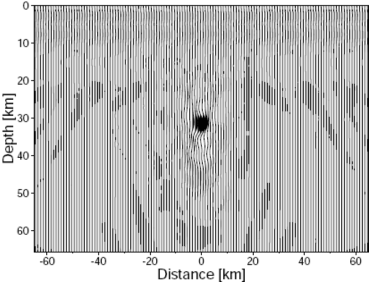

Ryberg&Weber (2000)

Require a high density of receivers:

Sodoudi et al. [2011]

A more general approach: migration

However:

Requires very good information on velocity model:
Too slow:

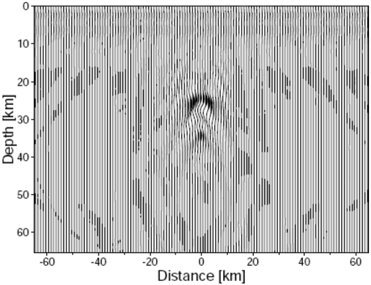

Ryberg&Weber (2000)

Require a high density of receivers:

Sodoudi et al. [2011]

A more general approach: migration

However:

Requires very good information on velocity model:
Too fast:

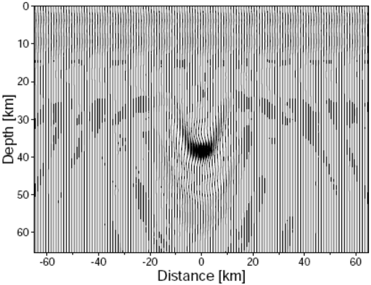

Ryberg&Weber (2000)

Require a high density of receivers:

Sodoudi et al. [2011]

A more general approach: migration

However:

Requires very good information on velocity model:
Too fast:

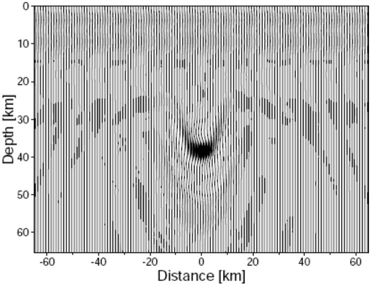

Ryberg&Weber (2000)

Get frowns & smiles

Require a high density of receivers:

Sodoudi et al. [2011]

However:

Requires very good information on velocity model:

Too fast:

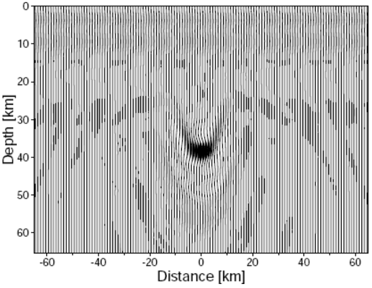

Ryberg&Weber (2000)

Get frowns & smiles

Require a high density of receivers:

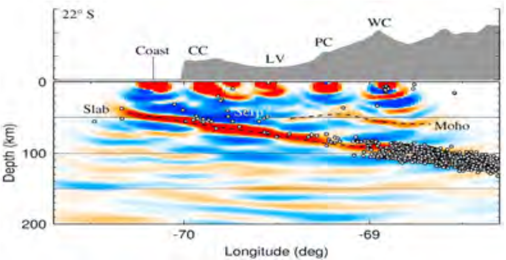

Sodoudi et al. [2011]

A more general approach: migration

However:

Requires very good information on velocity model:
Too fast:

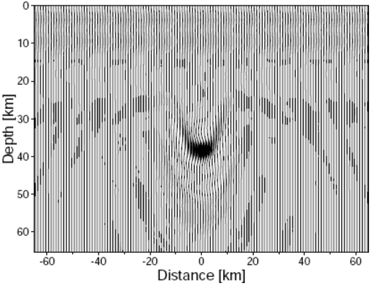

Ryberg&Weber (2000)
Get frowns & smiles

Require a high density of receivers:

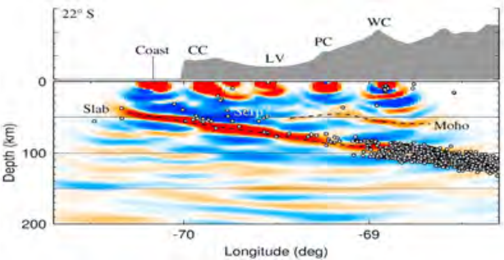

Sodoudi et al. [2011]
Otherwise: more smiles!

Effect of gradual transitions and frequency dependence

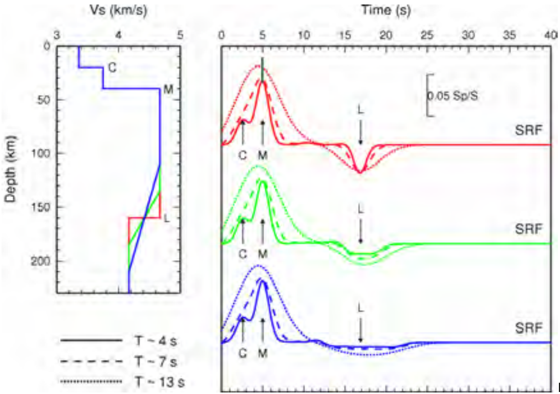

Kind et al. [2012]

- At long periods Moho peak shifted because of interference with intra-crustal (Conrad) discontinuity
- Transitional discontinuity (here LAB) disappears
- In addition to 1D effects shown, 2D - 3D effects can influence frequency dependence

Not covered because of lack of time:

- Waveform inversion (1D, 2D, 3D)

P - RF CCCP - discontinuities shown

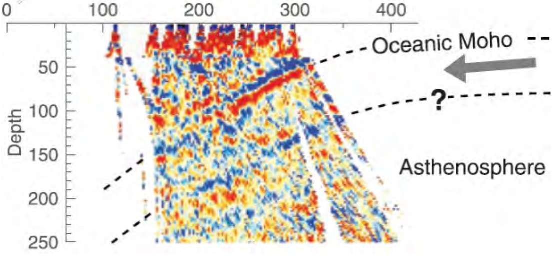

Japan [Kawakatsu et al., 2009]

Inversion - actual velocity diff wrt reference shown

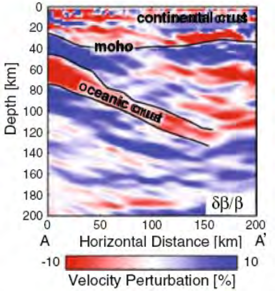

Cascadia [Rondenay, 2009]

- Deconvolution methods and sidelobes

Summary (of sorts)

P receiver functions - high-to-medium frequency

- Crustal and slab imaging ⇒ CCCP imaging/migration with direct conversion, maybe supplementary use of multiples
- Average crustal velocities ⇒ $H - \kappa$-stacking
- Detailed crustal velocity model ⇒ 1D waveform inversion (in combination with surface wave dispersion from ambient noise)
- 'Slab' velocity model: ⇒ 2D, 3D waveform inversion

P receiver functions - medium-to-low frequency

- Target: Mantle transition zone (410, 660 discontinuites) ⇒ Station or CCCP stacking with direct conversions)

S receiver functions - low frequency

- Mantle lithosphere imaging (lithosphere-asthenosphere-boundary (LAB) - mid-lithopheric discontinuities (MLD)

Pay attention to:

- Artifacts from in- and out-of plane diffractions, processing
- Separation of primaries from multiples

RF-methods sensitive to discontinuities not absolute velocities - subject to velocity-depth tradeoff!

References I

R. C. Aster, B. Borchers, and C. H. Thurber. *Parameter estimation and inverse problems*. Elsevier, 1st edition, 2005.

H. Kawakatsu, P. Kumar, Y. Takei, M. Shinohara, T. Kanazawa, E. Araki, and K. Suyehiro. Seismic evidence for sharp lithosphere-asthenosphere boundaries of oceanic plates. *Science*, 324:499–502, 2009. doi: 10.1126/science.1169499.

B. Kennett. *The seismic wavefield*, volume II: Interpretation of seismograms on regional and global scales. Cambridge University Press, 2002.

R. Kind and H. Yuan. *Encyclopedia of Solid Earth Geophysics*, chapter Seismic Receiver Function Technique, pages 1258–1269. Springer, 2011.

R. Kind, X. H. Yuan, and P. Kumar. Seismic receiver functions and the lithosphere-asthenosphere boundary. *Tectonophysics*, 536:25–43, April 2012. doi: 10.1016/j.tecto.2012.03.005.

C.A. Langston. Structure Under Mount Rainier, Washington, Inferred From Teleseismic Body Waves. *J. Geophys.Res.*, 84:4749–4762, 1979.

D. Lombardi, Braunmiller J., E. Kissling, and D. Giardini. Moho depth and Poisson's ratio in the Western?Central Alps from receiver functions. *Geophys. J. Int.*, 2008. doi: 10.1111/j.1365-246X.2007.03706.x.

J. Nábělek, Hetényi G., J. Vergne, S. Sapkota, B. Kafle, M. Jiang, H. Su, J. Chen, B. S. Huang, and Hi-Climb-Team. Underplating in the Himalayan-Tibet collision zone revealed by the Hi-CLIMB experiment. *Science*, 325:1371–1374, 2009. doi: 10.1126/science.1167719.

E. J. Rindraharisaona, F. Tilmann, X. Yuan, G. Rümpker, J. Giese, G. Rambolamanana, and G. Barruol. Crustal structure of southern Madagascar from receiver functions and ambient noise correlation: Implications for crustal evolution. *J. Geophys. Res.*, 122(2):1179–1197, 2017. doi: 10.1002/2016jb013565.

References II

S. Rondenay. Upper mantle imaging with array recordings of converted and scattered teleseismic waves. *Surv. Geophys.*, 30:377–405, 2009. doi: 10.1007/s10712-009-9071-5.

F. M. Schneider, X. Yuan, B. Schurr, J. Mechie, C. Sippl, C. Haberland, V. Minaev, I. Oimahmadov, M. Gadoev, N. Radjabov, U. Abdybachaev, S. Orunbaev, and S. Negmatullaev. Seismic imaging of subducting continental lower crust beneath the pamir. *Earth Planet. Sci. Let.*, 375:101–112, 2013. doi: 10.1016/j.epsl.2013.05.015.

F. Sodoudi, X. Yuan, G. Asch, and R. Kind. High?resolution image of the geometry and thickness of the subducting nazca lithosphere beneath northern Chile. *J. Geophys. Res.*, 116:B04302, 2011. doi: 10.1029/2010JB007829.

TRANSALP Working Group. First deep seismic reflection images of the eastern alps reveal giant crustal wedges and transcrustal ramps. *Geophys. Res. Let.*, 29, 2002. doi: 10.1029/2002GL014911.

L. P. Vinnik. Detection of waves converted from P to SV in the mantle. *Phys. Earth Planet. Int.*, 15:39–45, 1977.

I. Wölbern and G. Rümpker. Limitations of $h - \kappa$ stacking: ambiguous results caused by crustal layering. *J. Seismol.*, 21:221–235, 2017. doi: 10.1007/s10950-016-9599-z.

Junmeng Zhao, Xiaohui Yuan, Hongbing Liu, Prakash Kumar, Shunping Pei, Rainer Kind, Zhongjie Zhang, Jiwen Teng, Lin Ding, Xing Gao, Qiang Xu, and Wei Wang. The boundary between the Indian and Asian tectonic plates below Tibet. *Proc. Nat. Acad. Sci.*, 107(25):11229–11233, 2010. doi: 10.1073/pnas.1001921107.

L. Zhu. Crustal structure across the San Andreas Fault, Southern California from teleseismic converted waves. *Earth Planet. Sci. Let.*, 179:183–190, 2000.

L. Zhu and H. Kanamori. Moho depth variation in southern California from teleseismic receiver functions. *J. Geophys. Res.*, 105(B2):2969–2980, 2000.